## Werk

**Jahr:** 1975
**Kollektion:** fid.geo
**Signatur:** 8 Z NAT 2148:41
**Digitalisiert:** Niedersächsische Staats- und Universitätsbibliothek Göttingen
**Werk Id:** PPN1015067948_0041
**PURL:** http://resolver.sub.uni-goettingen.de/purl?PPN1015067948_0041

**LOG Id:** LOG_0043
**LOG Titel:** Characteristics of Azimuth independent optimum velocity filters designed for two-dimensional arrays
**LOG Typ:** article

## Übergeordnetes Werk

**Werk Id:** PPN1015067948
**PURL:** http://resolver.sub.uni-goettingen.de/purl?PPN1015067948
**OPAC:** http://opac.sub.uni-goettingen.de/DB=1/PPN?PPN=1015067948



## Contact

Niedersächsische Staats- und Universitätsbibliothek Göttingen
Georg-August-Universität Göttingen
Platz der Göttinger Sieben 1
37073 Göttingen
Germany
Email: gdz@sub.uni-goettingen.de

J. Geophys. 41, 265–279, 1975

# Characteristics of Azimuth Independent Optimum Velocity Filters Designed for Two-Dimensional Arrays

P. Hubral

Bundesanstalt für Bodenforschung, Hannover

Received April 11, 1974; Revised Version August 19, 1974

*Abstract.* The design of azimuth independent optimum velocity filters for arbitrary two-dimensional arrays is simplified with zero-order Bessel functions. Similarities with optimum velocity filters for one-dimensional arrays are discussed. An adequate choice of the array origin is recommended as it results in minimum length filter components. Simplifications for the computation and analysis of optimum velocity filters are provided for centre-symmetric array patterns. Computational experiments are performed on filters to characterize their performance on a large class of likely input signals. Features which can be related to the twodimensional wavenumber response of the array are described. The filters permit a control of the signal-to-noise ratio in the filtered output. It is shown that an increase in this ratio is only obtained at the expense of basically two types of signal distortion.

*Key words:* Optimum Multichannel Wiener Filters — Optimum Velocity Filters — Array Geometry — Frequency-Wavenumbers Domain — Filter Characteristics.

## *1. Introduction*

The particular type of velocity filters investigated in this work is based on the theory of optimum multichannel Wiener filters. Such a theory exists for continuous (Wiener, 1949; Robinson, 1962) and discrete filters (Robinson, 1967; Treitel, 1970). Velocity filters designed for two-dimensional arrays with the use of the continuous multichannel Wiener theory were first described by Burg (1964). Suboptimum velocity filters for one-dimensional arrays are discussed by Foster, Sengbush and Watson (1964). Optimum velocity filters for one-dimensional arrays are treated by Sengbush and Foster (1968), who compare their superior characteristics with various other velocity filters as suboptimum doublet filters (Foster *et al.*, 1964) and pie-slice filters (Embree, Burg and Backus, 1963). A critical analysis of optimum velocity filters with regard to their successful application to two-dimensional marine reflection data is given by Cassano and Rocca (1974). Superior characteristics of optimum velocity filters and the possibility to control the signal-to-noise ratio of the filtered output are the main reasons which led to the design of three-dimensional optimum velocity filters (Hubral, 1972). In the three-dimensional case various velocity filter designs are possible. It is the azimuth independent type which is shortly reviewed and subsequently characterized here. Examples are given to describe transfer characteristics and resolution of computed filters. An approximate relationship between the wavenumber response (Krey and Toth, 1973) of an array and the threedimensional Fourier transform of velocity filters for the same array is established. The control which can be exercised on the signal-to-noise ratio of the filtered output is investigated with the help of computational experiments. Some general rules for the use of the filters are established, which should be considered in their application.

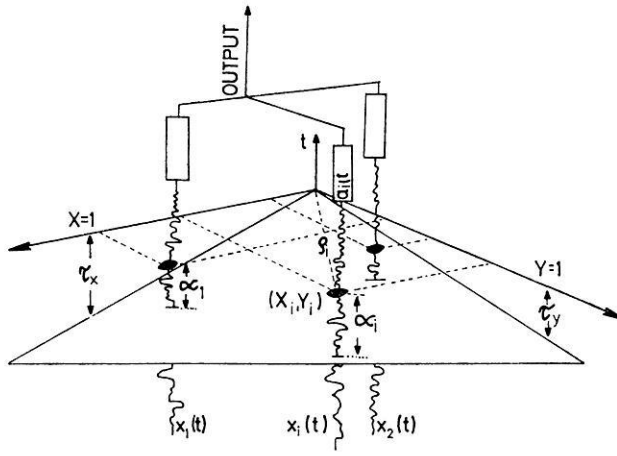


Fig. 1. Array pattern in $(x,y)$ plane and recorded traces indicating the moveout plane $t = -\tau_x x - \tau_y y$

## 2. *Theory*

The following stochastic model for actual seismic traces recorded at $N$ arbitrary detector locations $(X_i, Y_i)$, $(i=1,\ldots,N)$ is assumed to be the input for the desired filter:

$$\begin{gathered} x_i(t) = s(t-\alpha_i) + c(t-\bar{\alpha}_i) + n_i(t);\ (i=1,\ldots,N) \\ \alpha_i = \tau_x X_i + \tau_y Y_i;\ \bar{\alpha}_i = \bar{\tau}_x X_i + \bar{\tau}_y Y_i \end{gathered} \tag{1}$$

$s(t)$ is the common signal in each trace, $c(t)$ the coherent noise and $n_i(t)$, $(i=1,\ldots,N)$ some uncorrelated noise, which may vary from trace to trace. The values $\alpha_i$, $(i=1,\ldots,N)$ are the relative moveouts of a desired plane wave with signal waveform $s(t)$. The values $\bar{\alpha}_i$, $(i=1,\ldots,N)$ are respectively the moveouts of an undesired coherent noise plane wave with signal $c(t)$. Rather than designing a filter $a_i(t)$, $(i=1,\ldots,N)$, (Fig. 1) for just one stochastic input model of form (1) it is assumed that an ensemble of input traces is to be optimally filtered into the signal $s(t)$. To achieve this, each ensemble member is allowed to differ only in the values $\tau_x$, $\tau_y$ (Fig. 1) and $\bar{\tau}_x$, $\bar{\tau}_y$ in such a way that all permitted plane waves from all azimuths fall into two apparent velocity ranges. The ensemble of signal plane waves is expected to fall into a velocity range refered to as the pass region, the ensemble of coherent noise waves into a range refered to as the reject region. The filter $a_i(t)$, $(i=1,\ldots,N)$ which is obtained with the assumption that all signals are broad band and all waves within pass and reject region may arrive at the array with equal likelihood is specified by the following normal equations (Hubral, 1972):

$$\sum_{i=1}^{N} A_i(f)[\Phi_{s_i s_j}(f) + \eta \Phi_{c_i c_j}(f) + \nu \Phi_{n_i n_j}(f)\,\delta_{ij}] = \Phi_{s s_j}(f);\ (j=1,\ldots,N) \tag{2}$$

$$\Phi_{s_i s_j}(f) = (1/2\pi \Delta r_0) \int_0^{2\pi} \int_{r_0-\Delta r_0/2}^{r_0+\Delta r_0/2} \exp\left(-2\pi i f r(\varrho_i \cos(\alpha-\xi_i) - \varrho_j \cos(\alpha-\xi_j))\right) d\alpha\, dr$$

$$\Phi_{c_i c_j}(f) = (1/2\pi \Delta r_0) \int_0^{2\pi} \int_{\bar{r}_0 - \Delta \bar{r}_0/2}^{\bar{r}_0 + \Delta \bar{r}_0/2} \exp\left(-2\pi i f r(\varrho_i \cos(\alpha - \xi_i) - \varrho_j \cos(\alpha - \xi_j))\right) d\alpha\, dr$$

$$\Phi_{s s_j}(f) = (1/2\pi \Delta r_0) \int_0^{2\pi} \int_{r_0 - \Delta r_0/2}^{r_0 + \Delta r_0/2} \exp\left(2\pi i f r \varrho_j \cos(\alpha - \xi_j)\right) d\alpha\, dr$$

$$\Phi_{n_i n_j}(f) = 1$$

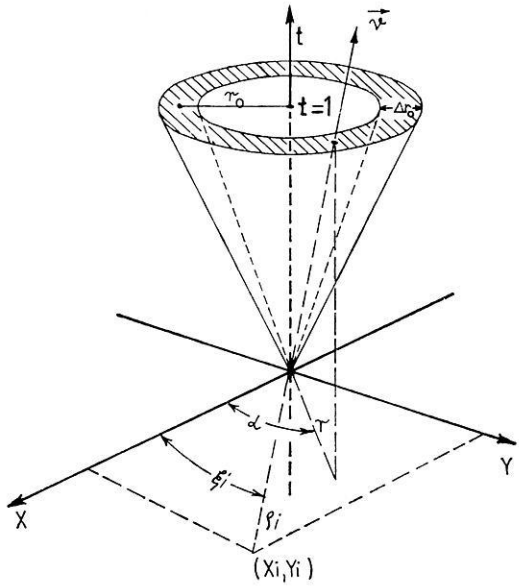


Fig. 2. Time domain cone featuring the limits of normal vectors of permitted moveout planes

$A_i(f)$, $(i = 1, \ldots, N)$ are the Fourier transforms of the wanted components $a_i(t)$, $(i = 1, \ldots, N)$ of the velocity filter. $\varrho_i$, $\xi_i$ are polar coordinates of the detector location i in respect to some as yet unknown coordinate origin within or outside the array. $r_0$ and $\Delta r_0$ are the moveout limits of the pass region. They are explained with the help of Fig. 2. Both values describe two inverted cones between which all normal vectors $\mathbf{v} = (\tau_x, \tau_y, 1)$ of the permitted input signal plane waves fall. $r$ in Fig. 2 is connected with $\tau_x$ and $\tau_y$ by the expression $r = \sqrt{\tau_x^2 + \tau_y^2}$. $\bar{r}_0$ and $\Delta r_0$ define the corresponding reject region for the coherent noise. Both, reject and pass region should not overlap with each other. $\eta$ and $\nu$ in (2) are arbitrary weighting factors influencing the signal-to-noise ratio of the filtered output. Noise weighting factors have been used in the context of various filter designs (Deregowski, 1971) with very good success. Their presence in optimum filter designs is justified by the fact that large noise weights cause increased rejection of the respective noise (Sengbush and Foster, 1968). Some negative side effects due to increasing $\eta$ and $\nu$ however exist and will be discussed later on. The solution of Eq. (2) is simplified with the help of zero-order Bessel functions as shown in the Appendix.

The $(f, k_x, k_y)$ transform is an ideal means of analysis (Burg,1964) to characterize a computed filter with regard to its performance on expected plane waves. It is used in this work to show the influence of various design parameters, as for instance the noise weighting factors and the recording patterns, on the filtered output. The $(f, k_x, k_y)$ domain of a computed filter is established as follows. The $N$ arbitrarily placed filter components $a_i(t)$, $(i=1,\ldots,N)$ at locations $X_i$, $Y_i$, $(i=1,\ldots,N)$ are used to define the following threedimensional operator:

$$a(t, x, y) = \sum_{i=1}^{N} a_i(t)\, \delta(x - X_i)\, \delta(y - Y_i)$$

Its Fourier transform is (Hubral, 1972)

$$A(f, k_x, k_y) = \sum_{i=1}^{N} A_i(f) \exp\left[-2\pi i(k_x X_i + k_y Y_i)\right] \tag{3}$$

This three-dimensional transform is periodic in $k_x$ and $k_y$ if detector locations fall onto a rectangular grid. The frequency response of any $\delta$-plane wave with the moveouts

$$\alpha_i = \tau_x X_i + \tau_y Y_i,\ (i = 1,\ldots,N;\ -\infty < \tau_x, \tau_y < +\infty)$$

can be expressed as:

$$R(f) = \sum_{i=1}^{N} A_i(f) \exp\left[-2\pi i f(\tau_x X_i + \tau_y Y_i)\right] \tag{4}$$

This function is obtained from (3) along the line $k_x = \tau_x f$, $k_y = \tau_y f$. If no filters are applied to the detector locations, the array acts only as a wavenumber filter (Krey and Toth, 1973). The function which is obtained by substituting $A_i(f) = 1$, $(i=1,\ldots,N)$ into (3) is commonly refered to as the wavenumber response of the array. It is shown with the help of an example that the wavenumber response, which is only determined by the array configuration, can strongly effect the characteristics one wants to force upon the array by designing a specific optimum velocity filter for it.

## *3. Array Geometry*

For any array and a specific pass and reject region the $(x,y)$ origin for the filter design can be chosen in such a way that the resulting filter length is small. This is of practical importance as it reduces the amount of computations for the design as well as the actual filtering process. The real input traces need then only approximate stationarity over a shorter time interval. Particular array symmetries can in addition reduce the size of the normal equations, speed up the filter computations and cause a zero-phase response for any plane wave arriving at the array. As many of the subsequent observations apply to most other velocity filters they are only briefly reviewed.

### 3.1. Choice of Origin

For a given array an infinite number of velocity filters can be computed for one and the same pass and reject region. This is achieved by just changing the $(x,y)$ origin in the filter design. Only one filter is optimum optimorum. Its origin should be selected in such a way that the largest of all resulting detector distances $\varrho_i$, $(i=1, \ldots,N)$ is at its minimum. This results in the shortest overall moveoutwidth of the pass and reject region within the array. It is easily seen in Fig. 1 that moving the $(x,y)$ origin to a place within the detectors reduces the moveouts $\alpha_i (i=1,\ldots,N)$. Filters should be as long as the largest moveout difference in the input. This has been shown by Galbraith and Wiggins (1968) for optimum stacking filters. These filters are in fact closely related to optimum velocity filters as shown by Hubral (1974). The choice of origin recommended here leads in the case of two-dimensional optimum velocity filters to the so-called 'centre-trace estimate' filter (Sengbush *et al.*, 1968). The maximum moveout difference for velocity filters in this work is $t_M = 2 r_{\max} \varrho_{\max}$, $r_{\max} = \mathrm{Max}(r_0 + \Delta r_0/2, \bar{r}_0 + \overline{\Delta r}_0/2)$. $r_{\max}$ is the maximum moveout value and $\varrho_{\max}$ the maximum detector distance of $\varrho_i (i=1,\ldots,N)$ from the origin. The choice of origin also affects the phase response of filters. This is shown in the next subsection.

### 3.2. Phase Response

The velocity filter transfer function for a specific broad band plane wave is given in expression (4). For an arbitrary array configuration and plane wave this is generally a complex function, thus indicating that both the amplitude of a plane wave signal and its phase is modified by the filter. As every increase in the phase of a signal affects a delay, plane waves arriving from various azimuths with even the same velocity may pass with different delays. This is generally undesired and can often be avoided by ensuring a zerophase response of the array for all possible plane waves. The velocity filter is then entirely characterized by the modulus of $A(f, k_x, k_y)$ as the phase of this transform is zero everywhere. This particular advantage is offered by centre-symmetric arrays. It is easily verified that the function (4) is real for any array configuration where for each detector location $(X_i, Y_i)$ another location $(-X_i, -Y_i)$ exists and both have the same symmetric filter component applied to it. That all filter components obtained from (2) are symmetric and the same for centre-symmetric pairs is verified by substitution.

### 3.3. Array Symmetry and Normal Equations

Centre-symmetric arrays not only provide simple phase relations, they also reduce the number of normal Eq. (2) and thus speed up the computation of filters considerably. For any centre-symmetric pair of detectors, the number of normal equations can be reduced by one. This can again be verified by substitution. Consequently those arrays may easily be computed where many detector positions fall centre-symmetrically on few concentric circles. In this case the number of normal equations corresponds then only to the number of circles.

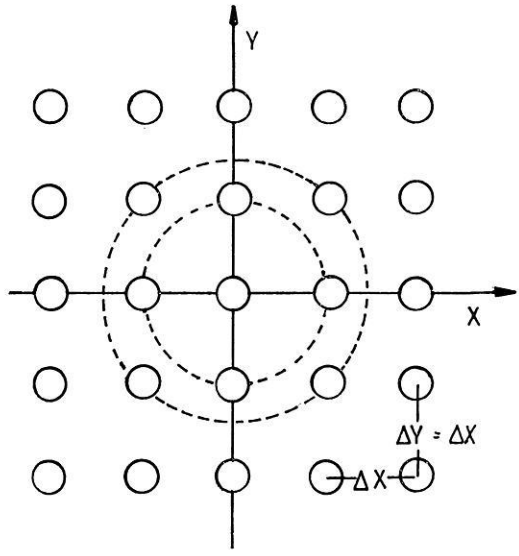


Fig. 3. Array pattern

### 4. *Computational Experiments*

Although filters are designed to possess azimuth independent transfer characteristics, the actual filter properties for certain array patterns are nevertheless often azimuth dependent. One example is subsequently discussed, where desired characteristics are well approximated. Another example is presented to point out a generally existing relationship between velocity filter characteristics and the wavenumber response of the array. The expected least square error as a function of the filter length (Treitel, 1970) is shown to be also useful in providing some indication about how well desired velocity filter characteristics are approximated by the actual filter. An investigation of the noise weighting factors $\eta$ and $\nu$ is done on some representative examples. Increasing the weighting factors reveals that increased attenuation of the noise has to be paid for with a deterioration of signal transfer characteristics. Increasing $\nu$ depresses the high frequency content of the filtered signals. Increasing $\eta$ causes a 'pushing effect' in the characteristics of the $(f, k_x, k_y)$ domain, which is explained below.

#### 4.1. Example

The array pattern is the rectangular $N \times N$ grid ($N=5$) of Fig. 3. As the 25 detectors can be considered to fall onto six concentric circles, the normal Eqs. (2) can be reduced to the sixth order. Additional design parameters are chosen as: $r_0=0.5$, $\Delta r_0=1.0$, $\nu=0.08$ and $\eta=0$. The time sampling period of the computed digital filter is $\Delta t=1$. The first quadrant of the three-dimensional $(f, k_x, k_y)$ diagram is shown in Fig. 4 at different levels of frequencies: $f=0, f=f_N/4, f=f_N/2, f=3f_N/4$ and $f=f_N$. $f_N=1/2\,\Delta t$ is the Nyquist frequency. The three-dimensional transform is periodic with the periods $k_x=1/\Delta x$, $k_y=1/\Delta y$ and $f=1/\Delta t$. Fig. 4 (lower right

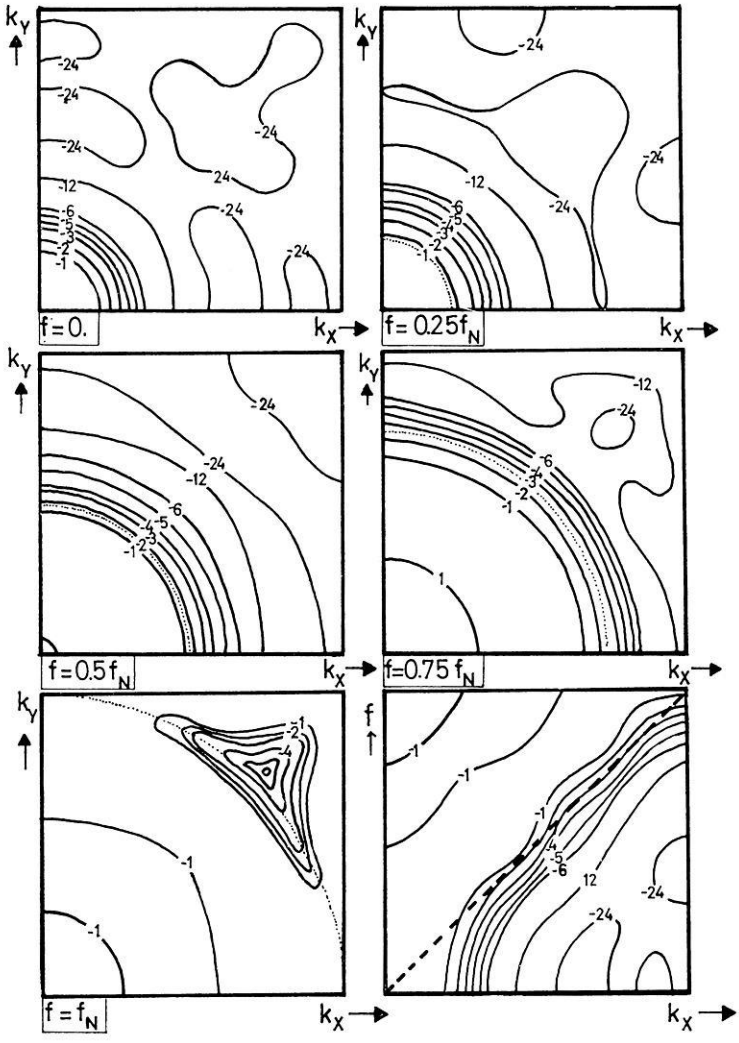


Fig. 4. Contours of the function $20 \log|A(f, k_x, k_y)/A_{\max}(f, k_x, k_y)|$ in the first quadrant $(0 \leq k_x \leq 1/2\,\Delta x,\ 0 \leq k_y \leq 1/2\,\Delta y,\ 0 \leq f \leq 1/2\Delta t)$ at different frequency levels

corner) shows the first quadrant in the plane $k_y = 0$. The limit of the circular cone is indicated as a straight dotted line. The area inside the cone represents the desired pass region in the $(f, k_x, k_y)$ domain in which all function values are expected to approximate $A(f, k_x, k_y) = 1$. Outside the cone is the reject region which should hopefully approach $A(f, k_x, k_y) = 0$.

The desired characteristics of this example are reasonably well approximated apart from frequencies near $f = 0$. This is typical for optimum velocity filters and has already been observed on one-dimensional arrays (Sengbush *et al.*, 1968). The desired circular shape of the characteristics is reasonably well maintained. If for instance the width between the —3 dB and —12 dB contours is defined as the resolution of the

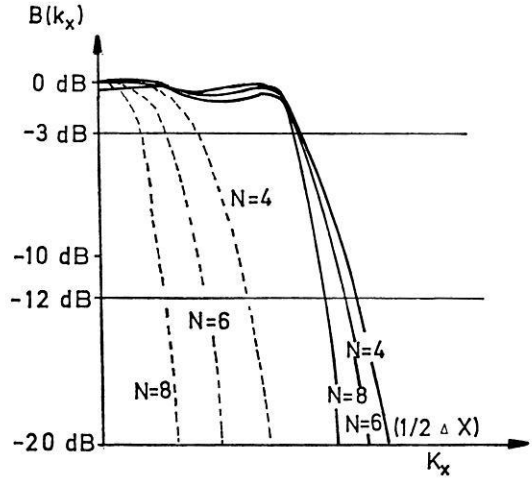


Fig. 5. Graphs of $B(k_x) = 20 \log |A(f_N/2, k_x, 0)/A_{\max}|$ for velocity filters (full lines) and straightforward stacks (dashed lines) as a function of the array size $N$

filter, one can state that this resolution is very much independent of frequencies and azimuths. To give some indication on how the resolution of the filter changes as a function of $N$, the values $A(f_N/2, k_x, 0)$ are displayed in Fig. 5 as a function of $k_x$ for $N=4$, $N=6$ and $N=8$. Fig. 5 also includes the corresponding function $A(f_N/2, k_x, 0)$ for the straight-forward stack. It can be seen that for the same $N$ the resolution of the filter is of the same order as for the straight stack. To verify this one only has to shift the respective curves for the same value of $N$ in Fig. 5 parallel to the $k_x$-axis to have their downward sloping part overlapped with each other.

### 4.2. Reluctance Tendancy

Certain arrays show a larger or smaller degree of reluctance towards approximating desired velocity filter characteristics. Some relationship can however be established between actually observed characteristics in the $(f, k_x, k_y)$ domain and the wave number response of the array. As seen by their wavenumber responses L-shaped and cross shaped arrays favour very much the directions of the array legs, while triangular or circular arrays reveal far less azimuth dependent characteristics. A summary of the characteristics of basic array patterns is given by Harjes and Henger (1973). As various computational experiments have shown, it is not possible to design azimuth independent optimum velocity filters for L-shaped or cross-shaped arrays as their wavenumber responses only favour specific directions. The following example elucidates this point. A velocity filter was designed for the cross array of Fig. 6 with all other design parameters being equal to the previous example. The first quadrant of $A(f, k_x, k_y)$ of the computed filter is shown in Fig. 7 for the frequencies $f=0$, $f=f_N/4$, $f=f_N/2$ and $f=3f_N/4$. Rather than the desired circular conic pass-region of the previous example, it is this time an inverted pyramidic pass region which is approximated by the actual filter of this example.

This shows that obviously a strong dependence of the characteristics exists on the directions of the cross-legs. A good understanding of wavenumber responses of

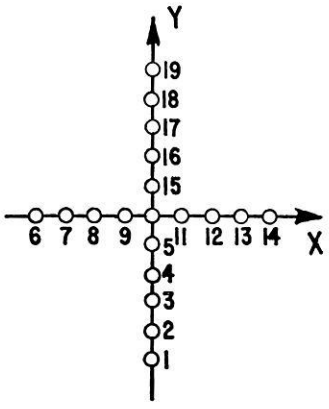


Fig. 6. Cross array

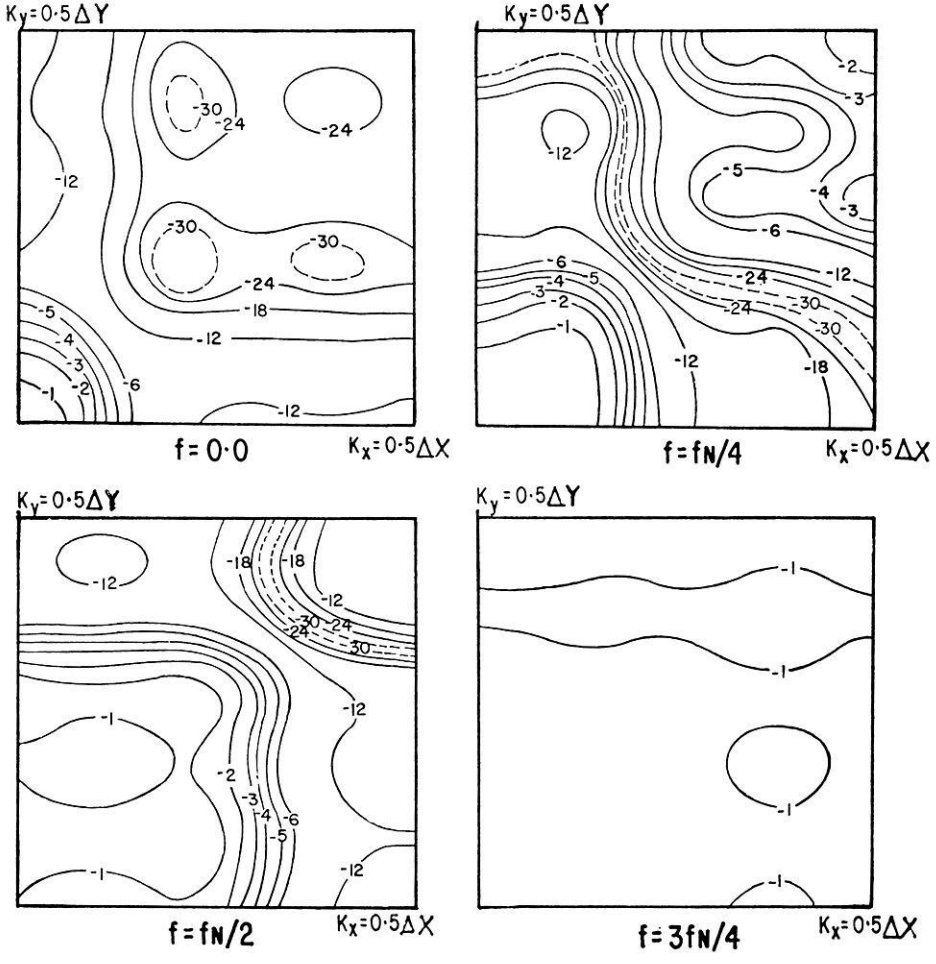


Fig. 7. Contours of $20 \log |A(f, k_x, k_y)/A_{\max}(f, k_x, k_y)|$ at different frequency levels

arrays can therefore be used to predict already to some extent the actually resulting but certainly more complex velocity filter characteristics. It is consequently not only the array size and the number of detectors, but also an inherent reluctance towards certain directions as already indicated by the wavenumber response which prevent actual characteristics of computed velocity filters from approximating desired ones. The (f, $k_x$, $k_y$) transform is a useful means of analysis of a velocity filter as one can obtain from it the array response for all possible plane waves. It can however still not provide any information with regard to the filter performance on uncorrelated noise nor can it be used to describe the signal-to-uncorrelated noise ratio of the filtered output. Other functions are equally useful to characterize velocity filters in this respect. This is shown in the next subsection.

### 4.3. Expected Errors

The expected error can provide some general qualitative indications about the performance of a computed filter. The basic operation which leads to the design of a filter, where the $N$ traces (1) are to be optimally filtered into the signal trace $s(t)$, is the minimization of the following least-square expression (Robinson, 1962):

$$E = \lim_{T\to\infty} \frac{1}{2T} \int_{-T}^{T} \left( s(t) - \sum_{i=1}^{N} a_i(t)^* x_i(t) \right)^2 dt \tag{5}$$

Substituting the computed filter together with the assumed model traces (1) into this expression provides the expected error (Treitel, 1972). The smaller this error, the better is the performance of the computed filter on the model traces.

The expected error can thus be investigated as a function of any filter design parameter (i.e. $(x,y)$ origin, detector locations, noise weighting factors, etc.). To demonstrate the usefulness of an expected error analysis, the first example of subsection 4.1 was again used and the normalized errors $E/E_{\max}$ were plotted as a function of the filter length and $r_{\max} = r_0 + \Delta r_0/2$. The results are shown in Fig. 8. They indicate that for all values $r_{\max}$ less than $\Delta t$ the expected errors approximate small values when increasing the filter length. From a certain length onwards there is no further reduction possible of the errors and computed filters perform from then on equally well on the specified ensemble of plane waves. It is obvious that for instance an increase of the incoherent noise enlarges the expected error. It is however not so obvious that increasing $r_{\max}$ to be greater than $\Delta t$ causes a similar effect (Fig. 8). The explanation for this is easily found as for $r_{\max} > \Delta t$ the conic pass region no longer fits into the basic period of the $(f, k_x, k_y)$ domain. Overlapping and partial cancellation of pass regions due to spatial periodicity of the $(f, k_x, k_y)$ transform cause then tremendous complexities which are commonly known as frequency and space aliasing effects. An indication of what can happen to optimum velocity filters for one-dimensional arrays due to space aliasing is provided by Sengbush and Foster (1968) and Cassano and Rocca (1974). The complexities they describe for one-dimensional arrays are larger in the case of two-dimensional arrays, particulary then, when array locations dont fall onto a rectangular recording grid and

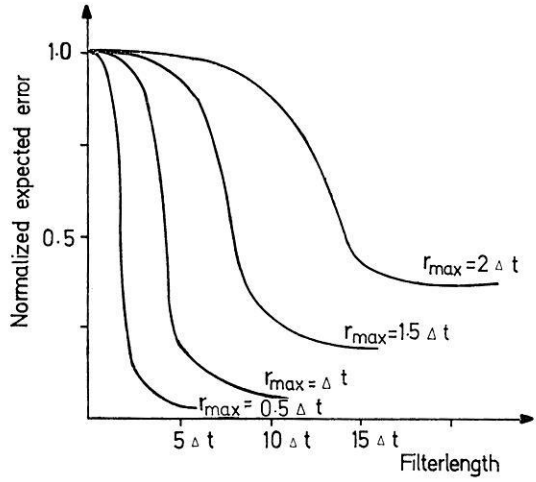


Fig. 8. Normalized expected errors as a function of the filter length

$A(f, k_x, k_y)$ is consequently not strictly periodic in $k_x$ and $k_y$. To avoid problems of wavenumber or space aliasing in the design, $r_{\max}$ should never be chosen to be larger than $\Delta t$ if detectors fall onto a grid with the spacing $\Delta x$. This is in correspondence with the conclusions arrived at by Sengbush and Foster (1968) for one-dimensional arrays.

### 4.4. The Noise Influence

It is assumed that the following random functions represent the ensemble of plane waves which arrive at the array locations $(X_i, Y_i)$, $(i=1,\ldots,N)$

$$x_j(t) = s(t-(\tau_x X_i + \tau_y Y_i)) + n_j(t)\ ;\ (j=1,\ldots,N)$$

The values $\tau_x$ and $\tau_y$ satisfy the condition $\sqrt{\tau_x^2+\tau_y^2}=r$. In addition the following equations are true for the power spectra of $s(t)$ and $n_i(t)$, $(i=1,\ldots,N)$

$$\Phi_{ss}(f) = \mathrm{rec}\,(f),\ \Phi_{n_i n_j}(f) = \mathrm{rec}\,(f)\,\delta_{ij},\ (i,j=1,\ldots,N)$$

$$\mathrm{rec}\,(f) = \begin{cases} 1 \text{ for } |f| \leq 1/2 \\ 0 \text{ for } |f| > 1/2 \end{cases}$$

The array locations are given by the array of Fig. 3. The velocity filter applied to the array is the one computed in subsection 4.1 for $N=6$.

The output power of the signals as a function of $r$ is subsequently refered to as $P(r)$ and the output power of the uncorrelated noise as $P_n$. The signal-to-uncorrelated noise ratio $P(r)/P_n$ as a function of the moveout $r$ for various weighting factors $\nu$ of the filter is shown in Fig. 9a. It is seen that the signal-to-uncorrelated noise ratio of the optimum velocity filter can be improved by as much as a factor of 2 for $\nu=300$. This improvement however decreases with increasing the moveout $r$. For

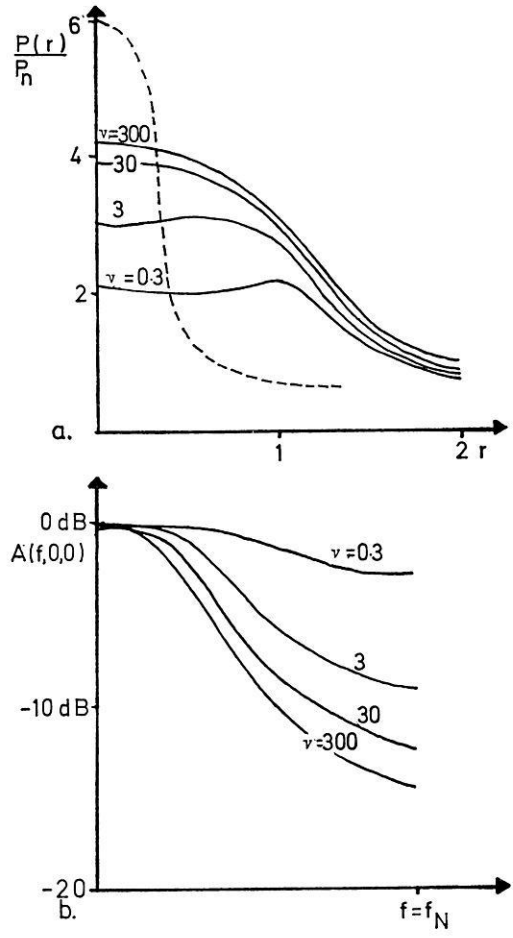


Fig. 9. a Signal-to-uncorrelated noise ratio as a function of moveout r. Dashed line corresponds to straight stack. b Values of $20 \log |A(f, k_x, k_y)/A_{\max}(f, k_x, k_y)|$ along the line $k_x = k_y = 0$

small moveouts $r$ the signal-to-noise ratio is never as good as in the straightforward stack, which is known to be the best incoherent noise rejector. The corresponding function representing a straight-forward addition is the dotted curve in Fig. 9a. From the graphs one can draw the interesting conclusion that one can obviously not have an optimum incoherent noise rejector and an optimum velocity filter (i. e. coherent signal pass- or reject filter) at the same time. A compromise between both extremes must and can be found by changing $\nu$. The optimum value of $\nu$ depends on the type of traces to be filtered. The increased rejection of uncorrelated noise has to be paid for with a loss in the high frequency content of the passed signals. This is shown in Fig. 9b for the same examples however only for $r = 0$. To complete the investigation of noise weighting factors, the influence of $\eta$ on the transfer characteristics is demonstrated with the help of one more example. A significant improvement of the signal-to-correlated noise ratio for broad band signals was observed by increasing $\eta$. The

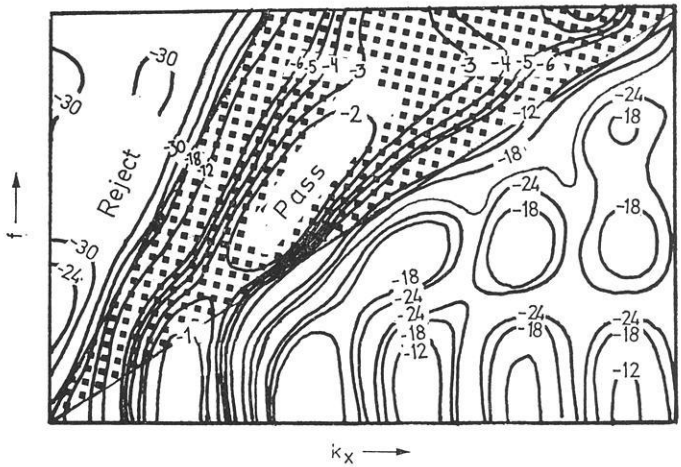


Fig. 10. Cross section of $20 \log |A(f, k_x, k_y)/A_{\max}(f, k_x, k_y)|$ of a pass-reject filter in the plane $k_y = 0$ for $0 \leq f \leq f_N$ and $0 \leq k_x \leq 1/2\Delta x$

improvement can be as much as a factor of 10. For marine reflection data and optimum velocity filters for one-dimensional arrays the optimum value of $\eta$ was found to fall between 0.5 and 2.0 (Cassano *et al.*, 1974). The increased rejection is again achieved at the expense of distorted signal characteristics. In particular it was observed that actual pass regions in the $(f, k_x, k_y)$ domain of a filter are increasingly pushed away from reject regions by enlarging $\eta$. This happens mainly at low frequencies and only up to a certain value of $\eta$. The low left corner in Fig. 10 gives a demonstration for this. The specific design parameters of the pass-reject filter are not given as they are not needed to explain the effect. For small values of $\eta$ and low frequencies the actual pass region moves towards the left and for large values of $\eta$ to the right. This interesting result which was constantly observed on various computed filters should by all means be considered, when applying computed filters to actual traces. Pass and reject signals for low frequencies which fall close to each other at the pass and reject limits are mostly influenced by the pushing effect and can cause an appreciable change of quality of the filtered traces.

## *Appendix*

Expression $\Phi_{s_i s_j}(f)$ can be simplified to

$$\Phi_{s_i s_j}(f) = (1/2\pi \Delta r) \int_0^{2\pi} \int_{r_0 - \Delta r_0/2}^{r_0 + \Delta r_0/2} \exp(2\pi i f r \, Rij \cos(\alpha - \lambda)) \, d\alpha \, dr$$

with

$$R_{ij}^2 = \varrho_i^2 + \varrho_j^2 - 2\,\varrho_i\,\varrho_j \cos(\xi_i - \xi_j)$$

and

$$\tan \lambda = (\varrho_i \sin \xi_i - \varrho_j \sin \xi_j)/(\varrho_i \cos \xi_i - \varrho_i \cos \xi_j)$$

This in turn can be written as

$$\Phi_{s_i s_j}(f) = \frac{1}{\Delta r_0} \int_{r_0 - \Delta r_0/2}^{r_0 + \Delta r_0/2} I_0(2\pi f r R_{ij}) dr$$

$I_0(r)$ is the zero-order Bessel function.

Substituting $p_0 = 2\pi f R_{ij}(r_0 - \Delta r_0/2)$ and $p_1 = 2\pi f R_{ij}(r_0 + \Delta r_0/2)$ leads to the further simplified expression:

$$\Phi_{s_i s_j}(f) = (1/2\pi R_{ij} f \Delta r_0) \cdot [\mathrm{Int}(p_1) - \mathrm{Int}(p_0)]$$

The zero-order Bessel function $I_0(r)$ and even its integral are often available as mathematical subroutines in a computer software library. If this is not the case one can expand $\mathrm{Int}(r)$ into a sufficiently long series of the form

$$\mathrm{Int}(r) = 2 \sum_{n=0}^{\infty} (-1)^n (r/2)^{2n+1} / ((2n+1) \cdot (n!)^2)$$

For expressions $\Phi_{c_i c_j}(f)$ and $\Phi_{s s_j}(f)$ one correspondingly can obtain the appropriate expressions:

$$\Phi_{c_i c_j}(f) = \frac{1}{\Delta \bar{r}_0} \int_{\bar{r}_0 - \Delta \bar{r}_0/2}^{\bar{r}_0 + \Delta \bar{r}_0/2} I_0(2\pi f r R_{ij}) dr$$

$$\Phi_{s s_j}(f) = \frac{1}{\Delta r} \int_{r_0 - \Delta r_0/2}^{r_0 + \Delta r_0/2} I_0(2\pi f r \varrho_j) dr$$

## *References*


Burg, J. B.: The application of the Wiener filter theory to the design of seismic arrays, S.E.G. Yearbook, p. 269, 1962

Burg, J. B.: Three-dimensional filtering with an array of seismometers. Geophysics *29,* 693–713, 1964

Cassano, E., Rocca, F.: After stack multichannel filters without mixing effects. Geophys. Prospecting *22,* 330–344, 1974

Deregowski, S. M.: Optimum digital filtering and inverse filtering in the frequency domain. Geophys. Prospecting *19,* 729–768, 1971

Embree, P., Burg, J. P., Backus, M. M.: Wide-band velocity filtering – the pie-slice process. Geophysics *28,* 948–974, 1963

Foster, M. R., Sengbush, R. L., Watson, R. J.: Design of suboptimum filter systems for multitrace seismic data processing. Geophys. Prospecting *12,* 173–191, 1964

Galbraith, J. N., Wiggins, R. A.: Characteristics of optimum multichannel stacking filters. Geophysics *33,* 36–48, 1968

Harjes, H. P., Henger, M.: Array – Seismologie. J. Geophys. *39,* 865–905, 1973

Hubral, P.: Three-dimensional optimum multichannel velocity filters, Geophys. Prospecting *21,* 29–45, 1972

Hubral, P.: Stacking filters and their characterisation in the (f–k) domain. Geophys. Prospecting *22,* 722–735, 1974
Krey, Th., Toth, F.: Remarks on wavenumber filtering in the field. Geophysics *38,* 959–970, 1973
Robinson, E. A.: Random wavelets and cybernetic systems. London: Griffin 1962
Robinson, E. A.: Statistical communication and detection with special reference to digital data processing of radar and seismic signals. London: Griffin 1967
Sengbush, R. L., Foster, M. R.: Optimum multichannel velocity filters. Geophysics *33,* 11–35, 1968
Treitel, S.: Digital multichannel filtering. Geophysics *35,* 785–811, 1970
Wiener, N.: Extrapolation, interpolation and smoothing of stationary time series. Technology Press of Mass. Inst. Techn., Cambridge, Mass., 1949

Dr. Peter Hubral
Bundesanstalt für Bodenforschung
D-3000 Hannover-Buchholz
Stilleweg 2
Federal Republic of Germany